



25th ABCM International Congress of Mechanical Engineering
October 20-25, 2019, Uberlândia, MG, Brazil

COB-2019-0659

APPROXIMATION OF THE INERTIAL EFFECTS OF AN ELASTO-VISCOPLASTIC MATERIAL IN A CAVITY

Giovanni Minervino Furtado

Federal University of Rio Grande do Sul, Department of Mechanical Engineering, Porto Alegre - RS, Brazil
giovannimf@mecanica.ufrgs.br

Márleson R. S. Ferreira

Federal University of Rio Grande do Sul, Department of Pure and Applied Mathematics, Porto Alegre - RS, Brazil
marleson.ferreira@ufrgs.br

Sérgio Frey

Federal University of Rio Grande do Sul, Department of Mechanical Engineering, Porto Alegre - RS, Brazil
frey@mecanica.ufrgs.br

Mônica F. Naccache

Paulo R. de Souza Mendes

Department of Mechanical Engineering, Pontifícia Universidade Católica, Rio de Janeiro - RJ, Brazil
naccache@puc-rio.br, pmendes@puc-rio.br

Abstract. *Viscoplastic fluids are materials of great interest both in industry and in our daily lives. These applications range from food and cosmetics products to industrial applications such as plastics in the industry of polymers and drilling muds in the oil industry. This class of material is characterized by having a yield stress that must be exceeded to the material starts to flow. These fluids are classically predicted by purely viscous models with yield stress. In the last decade, however, there some experimental visualizations has reported that the unyielded regions exhibit elasticity inside. This work is an attempt to investigate the effect of elasticity and inertia in those materials. It was studied, therefore, inertia flow of elastic-viscoplastic materials with no thixotropic behavior, according to the material equation introduced in de Souza Mendes (2011). The mechanical model is approximated by a stabilized finite element method in terms of extra stress, pressure and velocity. Due to its fine convergence feature, the method allows the use of equal-order finite elements and generates stable solutions in high advective-dominated flows. In this study is considered the geometry of a biquadratic cavity, in which the top wall moves to the right with constant velocity. In all computations is used biquadratic Lagrangian (Q1) elements. Results focuses in determining the influence of the flow intensity and inertia on the position and shape of unyielded regions. These results proved to be physically meaningful, indicating a strong interlace between flow intensity and inertia on determining of the topology of yield surfaces.*

Keywords: *elastic-viscoplastic materials, finite element, biquadratic cavity, elasticity and inertia*

1. INTRODUCTION

Elasto-viscoplastic fluids are structured materials that exhibit a complex non-Newtonian behavior that is related to their structure state, which, in turn, depends on the level of stress applied to it. Below a certain stress limit, called the yield stress, the material is highly structured, with high levels of elasticity and viscosity. This region can be called a apparently unyielded regions. When subjected to stress levels above the flow value, the material undergoes a rupture leading to a fluid-like behavior, where the viscosity decays in order of magnitude and their elasticity tends to disappear and these regions are called apparently yielded regions. Recent experiments report results showing some elastic effect on viscoplastic fluid flow (de Souza Mendes, 2007; Sikorski *et al.*, 2009). This class of material is present in several important industrial sectors such as petroleum, food products and cosmetics. Therefore, the modeling of its complex nonlinear mechanical behavior is of extreme industrial relevance for the prediction and understanding of these different processes.

In this work, a steady-state elasto-viscoplastic fluid flow is performed. In the momentum equation, the advective term is preserved in order to evaluate the inertial effects on the flows. In order to consider the elasticity below the yield stress

and a pseudoplastic behavior above the yield stress, a modification of the Oldroyd-B model equation is also employed. However, this Oldroyd-B type model does not consider the structure of the fluid and has not been tested in simple flow. More recently, a new and more reliable constitutive equation of the Oldroyd-B type was proposed in Nassar *et al.* (2011). An important feature of this equation is that it is also able to predict the thixotropic behavior of fluids, a feature that may be present in many viscoplastic materials. This model is more representative than that used in Martins *et al.* (2013), since it involves the determination of a structure parameter to describe the microstructure of the fluid. The structure parameter is evaluated with the aid of an additional (hyperbolic) equation that must be solved together with the conservation equations and the constitutive equation. The numerical solutions of conservation and government equations were obtained using a formulation of three Galerkin least squares (GLS) fields, which takes into account the fields of velocity, pressure and extra-stress as prime variables (Behr *et al.*, 1993). This formulation can be seen as an extension - for the elasto-viscoplastic case subject to shear-thinning of the relaxation and retardation times, and the viscoplastic SMD function (de Souza Mendes *et al.*, 2007) - of the formulation proposed in Behr *et al.* (1993), for fluids of constant viscosity. Thus, the numerical results of inertial flows of elasto-viscoplastic fluids are obtained within a lid-driven cavity and a discussion about the inertial effects and the flow intensity on the morphology of the apparently unyielded regions is presented.

2. THE MECHANICAL MODEL

For the flow of elasto-viscoplastic material can be modeled by the following governing equations,

$$\rho \frac{d\mathbf{u}}{dt} = -\nabla p + \nabla \cdot \boldsymbol{\tau} + \rho \mathbf{g}, \quad (1)$$

$$\nabla \cdot \mathbf{u} = 0 \quad (2)$$

where $d(\cdot)/dt \equiv \partial(\cdot)/\partial t + \mathbf{u} \cdot \nabla(\cdot)$ is the material derivative, ∇ is the gradient operator, \mathbf{u} is velocity vector, ρ is the fluid density, \mathbf{g} is the gravitational force per unit mass, p is the pressure field and $\boldsymbol{\tau}$ is the extra stress tensor.

To model the elasto-viscoplastic behavior of the material, the extra stress tensor is described by an Oldroyd equation that takes into account not only elasticity, but also viscoplasticity and thixotropy. The constitutive equation of the model adopted in this work was proposed by de Souza Mendes (2007), which follows the following relation:

$$\boldsymbol{\tau} + \theta_1(\dot{\gamma}) \overset{\nabla}{\boldsymbol{\tau}} = 2\eta(\dot{\gamma})(\mathbf{D}(\mathbf{u}) + \theta_2(\dot{\gamma}) \overset{\nabla}{\mathbf{D}}(\mathbf{u})), \quad (3)$$

where $\dot{\gamma} = \sqrt{2\text{tr}[\mathbf{D}(\mathbf{u})]^2}$ is the magnitude of the strain rate tensor, \mathbf{D} is the strain rate tensor and $\overset{\nabla}{\boldsymbol{\tau}}$ and $\overset{\nabla}{\mathbf{D}}$ represent the upper convected derivatives, respectively given by:

$$\overset{\nabla}{\boldsymbol{\tau}} = (\nabla \boldsymbol{\tau})\mathbf{u} - (\nabla \mathbf{u}) \cdot \boldsymbol{\tau} - \boldsymbol{\tau} \cdot (\nabla \mathbf{u})^T \quad (4)$$

$$\overset{\nabla}{\mathbf{D}} = (\nabla \mathbf{D})\mathbf{u} - (\nabla \mathbf{u}) \cdot \mathbf{D} - \mathbf{D} \cdot (\nabla \mathbf{u})^T \quad (5)$$

The differential equation of the extra stress tensor is the standard Oldroyd-B viscoelastic model, except that structural viscosity, η , relaxation time, θ_1 , and retardation time, θ_2 , are dependent parameters. The evolution of the structure parameter is governed by a kinetic equation, with its material derivative in time given by:

$$\frac{d\lambda}{dt} = \frac{1}{t_{eq}} \left[(1 - \lambda) - (1 - \lambda_{eq}) \frac{\lambda}{\lambda_{eq}} \right] \quad (6)$$

where λ_{eq} is the equilibrium parameter, t_{eq} is equilibrium time, which is a time scale for the microstructure buildup (Link *et al.*, 2015). The imbalance between the building term, $\frac{1}{t_{eq}}(1 - \lambda)$, and the breakdown term, $\frac{1}{t_{eq}}(1 - \lambda_{eq})(\lambda/\lambda_{eq})$, determines whether the material will undergo aging or a rejuvenation process.

The equilibrium viscosity adopted is a function of the stress when the fluid is apparently flowing characterized by a high finite viscosity at the limit where $\dot{\gamma} \rightarrow 0$, given by de Souza Mendes (2007):

$$\eta_{eq}(\dot{\gamma}) = \left[1 - \exp\left(\frac{-\eta_0 \dot{\gamma}}{\tau_y}\right) \right] \left[\frac{\tau_y}{\dot{\gamma}} + K \dot{\gamma}^{n-1} \right] + \eta_\infty, \quad (7)$$

where η_0 is the low shear rate viscosity plateau, τ_y is the yield stress, K is the consistency index, n is the power-law index, and η_∞ is the high shear rate viscosity plateau.

The relaxation time and retardation, respectively used are defined:

$$\theta_1 = \left(1 - \frac{\eta_\infty}{\eta_{eq}} \right) \frac{\eta_{eq}}{G_{eq}}, \quad (8)$$

$$\theta_2 = \left(1 - \frac{\eta_\infty}{\eta_{eq}} \right) \frac{\eta_\infty}{G_{eq}}. \quad (9)$$

$$(10)$$

The elastic modulus in equilibrium, G_{eq} , is defines as

$$G_{eq}(\lambda_{eq}) = G_0 \exp\left(m \frac{1}{\lambda_{eq}} - 1\right), \quad (11)$$

where G_0 represents the shear modulus of the material in its fully structured state and m a dimensionless positive constant that governs the sensitivity of G_{eq} to the structuring level. This function is used to predict the elastic behavior of viscoplastic fluids only in regions where the stress level is lower than the flow stress.

As η_∞ , the low viscosity region corresponds to the retardation time is practically zero and the relaxation time is reduced to:

$$\theta_{eq} = \frac{\eta_{eq}}{G_{eq}}, \quad (12)$$

and the relationship between the equilibrium structure parameter and the equilibrium viscosity is given by,

$$\lambda_{eq}(\dot{\gamma}) = \frac{\ln \eta_{eq}(\dot{\gamma}) - \ln \eta_\infty}{\ln \eta_0 - \ln \eta_\infty} \quad (13)$$

3. GEOMETRY AND BOUNDARY CONDITIONS

The geometry considered is shown in Fig. 1. It consists of a unit cavity of length ($L_c = 1$) with the upper wall moving with constant velocity ($u_1 = u_c$; $u_2 = 0$) and its other walls and the two points of singularity in the two upper corners of the cavity subjected to non-slip and impermeable conditions ($u_1 = u_2 = 0$). All results were obtained using Lagrangian bi-linear interpolations (Q1) for all primary variables.

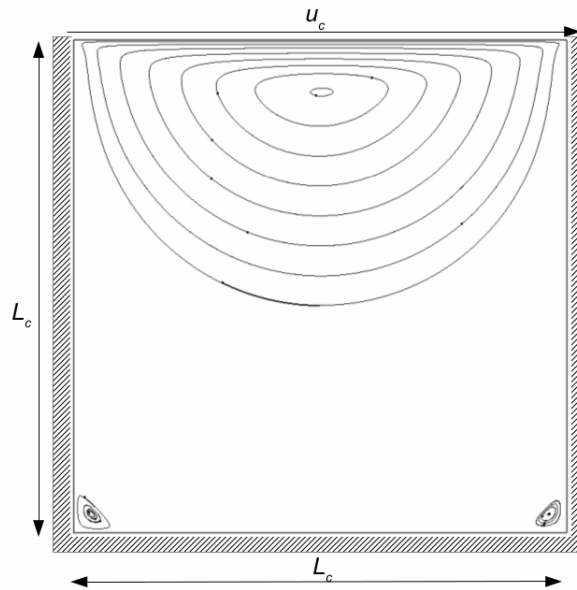


Figure 1. Geometry and boundary conditions

In Fig. 1 can be seen three recirculation regions, one central region associated with the main flow and two secondary regions in the lower corners of the cavity. These regions are caused by the effect of velocity on the cavity cover and will always be present in this geometry under the contour conditions discussed above.

4. DIMENSIONLESS PARAMETERS

The non-dimensionalization of the problem in accordance with de Souza Mendes (2007). To this end it is employed the characteristic shear rate $\dot{\gamma}_1$, defined as

$$\dot{\gamma}_1 \equiv \left(\frac{\tau_y}{K}\right)^{(1/n)}. \quad (14)$$

It is worth noting that $\dot{\gamma}_1$ is a purely rheological quantity, marking the beginning of the power-law region in the flow curve. The dimensionless counterparts of the problem variables are

$$\begin{aligned} t^* &= \dot{\gamma}_1 t; & \mathbf{x}^* &= \frac{\mathbf{x}}{L_c}; & \nabla^* &\equiv L_c \nabla; & \mathbf{u}^* &= \frac{\mathbf{u}}{\dot{\gamma}_1 L_c}; & \theta_{eq}^* &= \dot{\gamma}_1 \theta_{eq}; & \theta_0^* &= \dot{\gamma}_1 \frac{G_0}{\eta_0}; & U^* &= \frac{u_c}{\dot{\gamma}_1 L_c} \\ p^* &= \frac{p}{\tau_y}; & \boldsymbol{\tau}^* &= \frac{\boldsymbol{\tau}}{\tau_y}; & G^* &= \frac{G}{\tau_y}; & \eta_{eq}^* &= \frac{\eta_{eq} \dot{\gamma}_1}{\tau_y}; & \rho^* &= \frac{\rho}{\tau_y / (\dot{\gamma}_1 L_c)^2}, \end{aligned} \quad (15)$$

where L_c is a characteristic length of cavity and U^* is the non-dimensional intensity flow. It is used the definitions given in Eq. (15) to rewrite the governing equations in dimensionless form. All the boundary conditions and most of the resulting dimensionless equations happen to preserve the original form of their dimensional counterparts, such that they are identical except for the * superscripts that appear to indicate the non-dimensionality of the scaled variables.

5. NUMERICAL APPROXIMATION

To approximate the mechanical model described above, a multi-field Galerkin least-squares formulation, in terms of velocity, pressure and extra-stress, is employed. This formulation may be viewed as a direct extension of the model introduced by Behr *et al.* (1993) for constant viscosity fluids, to flows of elasto-viscoplastic materials. Proposed by Hughes *et al.* (1986) for Stokes flow, and later extended by Franca and Frey (1992) for Navier-Stokes flow, this formulation has been successfully applied to many engineering applications.

This model overcomes the shortcomings present in classical Galerkin approximations for fluid problems of interest, primarily, the need to satisfy functional compatibility conditions among the finite element subspaces of its primal variables. The model produces stable and meaningful approximations for fluid problems of interest that are exempt from numerical pathologies, even employing equal-order combinations of Lagrangean finite elements (for details, see Franca and Frey (1992) and Behr *et al.* (1993) and references therein). Exploiting such a feature in all of the computations shown in the upcoming numerical section, an equal-order bi-linear (Q1) finite element interpolation is used. More details of the numerical formulation are found in dos Santos *et al.* (2011).

6. NUMERICAL RESULTS

The results aim to study the effect of inertia on the flow pattern of viscoplastic materials subject to elasticity, by determining the morphology and position of their apparently unyielded regions.

It is worth noting that the following results are obtained for the steady state case (i.e. $\partial(\cdot)/\partial t \equiv 0$). Thus, the evaluation of the effects caused by inertia is due to the advective term of the momentum equation.

6.1 Mesh quality

To ensure that the numerical approximation is independent of the mesh used, the cross-sectional profile, at $x_1^* = 0.5$, of the magnitude of the extra stress, $\tau = (\tau_{ij}^2/2)^{1/2}$, for 4 meshes of bilinear elements was evaluated, as shown in Fig. 2. The M1 mesh with 900 Q1 elements, the M2 mesh with 2500 Q1 elements, the M3 mesh with 4900 Q1 elements and M4 mesh with 10,000 Q1 elements.

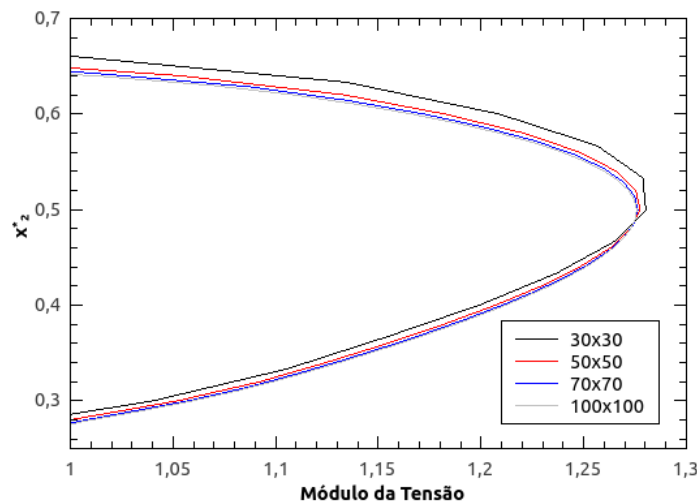


Figure 2. Mesh quality test: M1= 30×30 , M2= 50×50 , M3= 70×70 , M4= 100×100 ,

According to the test performed, in which the governing parameters used were $U^* = 0.1$, $\theta_0^* = 100$, $n = 0.5$, $m = 20$, $\tau_y = 1$, $\rho^* = 500$ as base case, for faster convergence. The M4 mesh (illustrated in Fig. 3) was chosen and employed for all cases investigated, since has a smaller error and it is the most refined mesh, whose error value is less than 2% compared to mesh M3, which means that the results are more accurate in the points of the elements of that mesh.

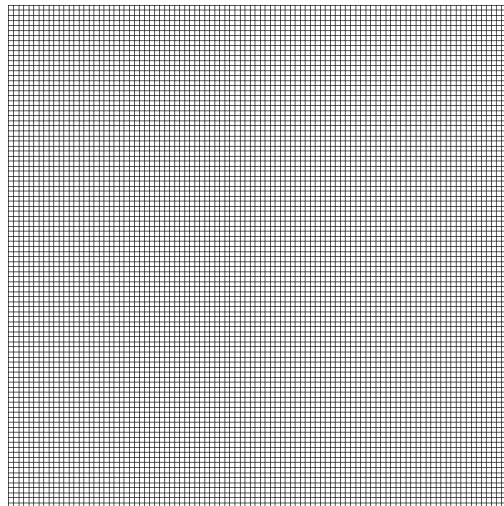


Figure 3. Finite element mesh (M4): 10,000 elements

6.2 Influence of flow intensity

The Fig. 4 shows the influence of the flow intensity on the flow surfaces. In these figures, the white zones represent yielded regions (when the shear rate exceed $\dot{\gamma}_1$) and the black zones represent the apparent unyielded regions (when the shear rate do not exceed $\dot{\gamma}_1$) of the flow. The support parameters were: $\theta_0^* = 100$, $n = 0.5$, $m = 20$, $\tau_y = 1$, $\rho^* = 500$.

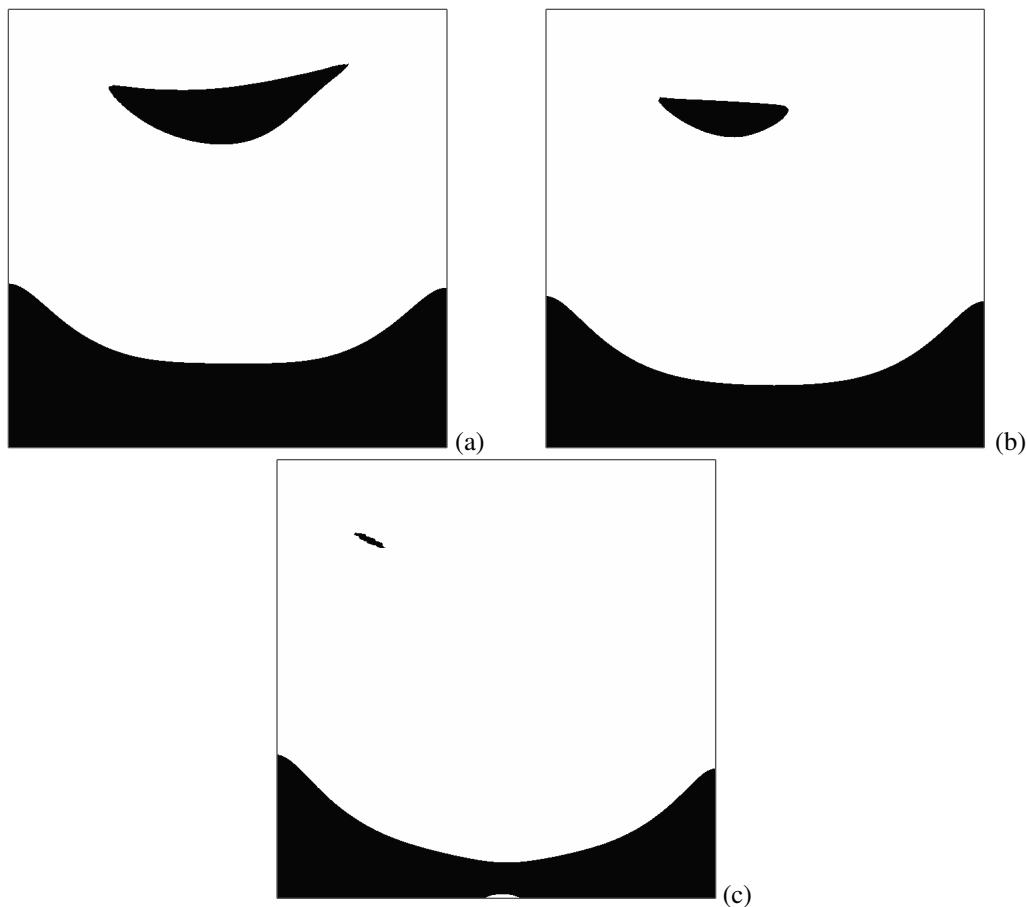


Figure 4. Yielded/unyielded regions for the support parameters: (a) $U^* = 0.05$, (b) $U^* = 0.1$, (c) $U^* = 0.2$

In Fig. 4 is perceived that as the flow intensity increases, the apparently unyielded regions decrease throughout the cavity. When the velocity is raised, there is a strong displacement of the apparently unyielded regions in the upper part of the cavity, this is due to the central vortex displacement. Thus, as intensity of flow increases, an increase in the effect of advection is noticed.

6.3 Influence of the inertia

On the other hand, the Fig. 5 shows the flow intensity under the variation of the inertial effects, using the following support parameters: $\theta_0^* = 100$, $n = 0.5$, $m = 20$, $\tau_y = 1$, $U^* = 0.15$. The parameter $U^* = 0.15$ was chosen because the inertial effects are more evident with a greater advection in the flow.

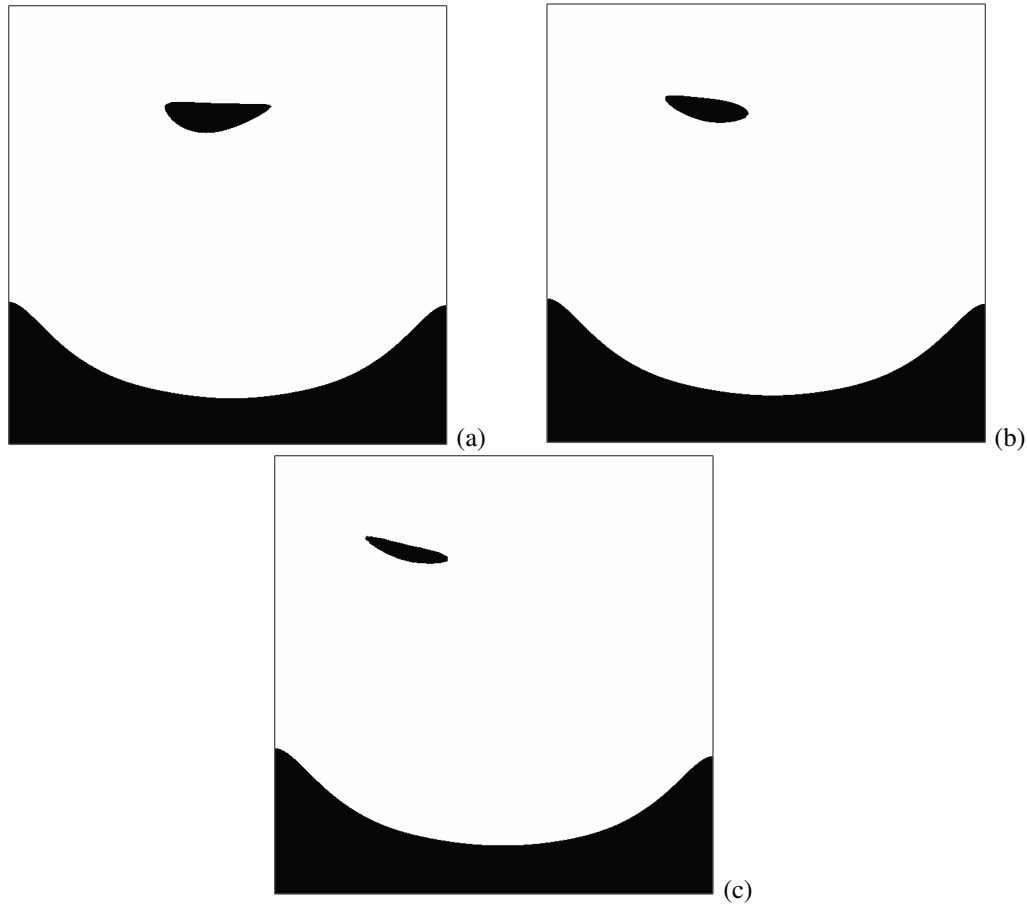


Figure 5. Yielded/unyielded regions for the support parameters: (a) $\rho^* = 50$, (b) $\rho^* = 300$, (c) $\rho^* = 500$

It is noticed in the Fig. 5 that the apparently unyielded regions decrease in every cavity with the increase of the inertial effect. In the lower part of the cavity, the inertial effect has little influence on the flow pattern, on the other hand, in the upper part, the flow pattern is strongly influenced by the inertial effect, since the main flow vortex suffers a large displacement to the right of the cavity according to the increase of the ρ^* .

7. CONCLUSIONS

In this work numerical simulations of elasto-viscoplastic flows were performed with the introduction of the inertial effects, where the geometry used was a forced cavity. The mechanical modeling was done using the mass conservation equation, the equation of the momentum coupled to an elasto-viscoplastic material equation proposed in Nassar *et al.* (2011). The mechanical model was approximated by a Finite Element method, namely the least squares Galerkin multi-field method in terms of extra-stress, pressure and velocity.

It was observed that the variation of the U^* , while holding $\rho^* = 500$, increases the advective effects on the flow. The apparently unyielded regions suffer a strong displacement to the right in the superior part of the cavity. On the other hand, holding $U^* = 0.15$, the variation of the inertial effects, ρ^* , has little influence on the flow pattern in the lower part, although, in the upper part, the flow pattern is strongly influenced by the inertial effects.

8. ACKNOWLEDGEMENTS

The authors acknowledge the brazilian funding agencies CAPES and CNPq for financial support.

9. REFERENCES

- Behr, M.A., Franca, L.P. and Tezduyar, T.E., 1993. “Stabilized finite element methods for the velocity-pressure-stress formulation of incompressible flows”. *Comput. Methods Appl. Mech. Eng.*, Vol. 104, pp. 31–48.
- de Souza Mendes, P.R., 2007. “Dimensionless non-Newtonian fluid mechanics”. *J. Non-Newtonian Fluid Mech.*, Vol. 147, No. 1-2, pp. 109–116.
- de Souza Mendes, P.R., 2011. “Thixotropic elasto-viscoplastic model for structured fluids”. *Soft Matter*, Vol. 7, pp. 2471–2483.
- de Souza Mendes, P.R., Naccache, M.F., Varges, P.R. and Marchesini, F.H., 2007. “Flow of viscoplastic liquids through axisymmetric expansions-contractions”. *J. Non-Newtonian Fluid Mech.*, Vol. 142, No. 1-3, pp. 207–217.
- dos Santos, D.D., Frey, S.L., Naccache, M.F. and de Souza Mendes, P.R., 2011. “Numerical approximations for flow of viscoplastic fluids in a lid-driven cavity”. *J. Non-Newtonian Fluid Mech.*, Vol. 166, pp. 667–679.
- Franca, L.P. and Frey, S.L., 1992. “Stabilized finite element methods: II. The incompressible Navier-Stokes equations”. *Comput. Meth. Appl. Mech. Eng.*, Vol. 99, pp. 209–233.
- Hughes, T.J.R., Franca, L.P. and Balestra, M., 1986. “A new finite element formulation for computational fluid dynamics: V. Circumventing the Babuška-Brezzi condition: a stable Petrov-Galerkin formulation of the Stokes problem accommodating equal-order interpolations”. *Comput. Methods Appl. Mech. Eng.*, Vol. 59, pp. 85–99.
- Link, F.B., Frey, S., Thompson, R.L., Naccache, M.F. and de Souza Mendes, P.R., 2015. “Plane flow of thixotropic elasto-viscoplastic materials through a 1:4 sudden expansion”. *Journal of Non-Newtonian Fluid Mechanics*, Vol. 220, pp. 162 – 174. ISSN 0377-0257. Viscoplastic fluids: From theory to application 2013.
- Martins, R.R., Furtado, G.M., dos Santos, D.D., Frey, S.L., Naccache, M.F. and de Souza Mendes, P.R., 2013. “Elastic and viscous effects on flow pattern of elasto-viscoplastic fluids in a cavity”. *Mechanics Research Communications*, Vol. 53, pp. 36–42.
- Nassar, B., de Souza Mendes, P.R. and Naccache, M.F., 2011. “Flow of elasto-viscoplastic liquids through an axisymmetric expansion–contraction”. *J. Non-Newtonian Fluid Mechanics*, Vol. 166, pp. 386–394.
- Sikorski, D., Tabuteau, H. and de Bruyn, J.R., 2009. “Motion and shape of bubbles rising through a yield-stress fluid”. *J. Non-Newtonian Fluid Mech.*, Vol. 159, pp. 10–16.

10. RESPONSIBILITY NOTICE

The authors are the only responsible for the printed material included in this paper.